

# U–Pb zircon dating by laser ablation-MC-ICP-MS using a new multiple ion counting Faraday collector array

Antonio Simonetti,<sup>\*a</sup> Larry M. Heaman,<sup>a</sup> Russell P. Hartlaub,<sup>a</sup> Robert A. Creaser,<sup>a</sup> Trevor G. MacHattie<sup>a</sup> and Christian Böhm<sup>b</sup>

<sup>a</sup> Department of Earth and Atmospheric Sciences, University of Alberta, Edmonton, Alberta, Canada. E-mail: antonio.simonetti@ualberta.ca; Fax: 1-780-492-2030; Tel: 1-780-492-4354

<sup>b</sup> Precambrian Mapping Section, Manitoba Industry, Economic Development and Mines, Winnipeg, Manitoba, Canada

Received 30th March 2005, Accepted 13th June 2005

First published as an Advance Article on the web 5th July 2005

This study reports U–Pb geochronological data for zircon obtained by laser ablation-multi-collector-ICP-MS using a new collector block design that includes three ion counters and twelve Faraday buckets. The collector configuration allows for simultaneous detection of ion signals from mass  $^{238}\text{U}$  to  $^{203}\text{Tl}$ , an important factor for the achievement of highly precise and reproducible Pb–Pb and Pb–U ratios. The main advantage of the multiple ion counting system is the capability to readily measure low Pb ion signals ( $<1 \times 10^6$  counts per second) resulting from single spot analyses of  $\leq 40$  microns (and corresponding small sample volumes). The latter is an extremely important feature when deciphering multiple domains in complexly zoned zircon populations. A comparative study was conducted between analytical protocols involving non-Tl- and Tl-doped laser ablation runs with regards to evaluating the external reproducibility (*i.e.*, relative standard deviation). The results indicate that the ( $2\sigma$ ) external reproducibility for both analytical protocols varies between  $\sim 0.3$ – $1.0\%$  for the  $^{207}\text{Pb}/^{206}\text{Pb}$ , and *ca.* 1.3 to  $<3.0\%$  for the  $^{206}\text{Pb}/^{238}\text{U}$  (and  $^{207}\text{Pb}/^{235}\text{U}$ ) values. The external reproducibility for the Pb/U values are relatively constant for the Tl-doped analyses, whereas those for the non-Tl runs are inversely correlated with the total absolute (Pb) count rates. The precision and accuracy of both analytical protocols were verified with the analysis of BR266 and 91500 zircon standards and zircons previously dated by ID-TIMS. The instrument configuration and Tl-doping protocol employed here are ideally suited for studies requiring the rapid analysis of a large number ( $n > 50$ ) of zircon grains.

## 1. Introduction

Isotope dilution-thermal ionization mass spectrometry (ID-TIMS) remains to date the method that yields the most accurate and precise U–Pb dates for accessory minerals. However, recent U–Pb studies of accessory minerals using laser ablation-inductively coupled plasma mass spectrometry (LA-ICP-MS) have made significant strides in generating precise and accurate ages.<sup>1,2</sup> LA-ICP-MS studies involving both quadrupole and, most recently, multicollector magnetic sector ICP instruments offer several advantages: 1–simple sample preparation procedures, 2–measurement of isotopic ratios at high spatial resolution (20 to 100  $\mu\text{m}$ ), 3–rapid analysis, typically of the order of several minutes, and 4–relative lack of expense when compared with costs incurred with other U–Pb analytical protocols, such as SHRIMP (sensitive high resolution ion microprobe) or ID-TIMS (isotope dilution-thermal ionization mass spectrometry). The availability of magnetic sector, multicollector-inductively coupled plasma mass spectrometry (MC-ICP-MS) technology has increased within the last decade, and has led to innovative research studies involving both stable and radiogenic isotope systems; the main reasons being the overall high ionization efficiency of the ICP source and simultaneous acquisition of ion beams having flat topped peak shapes. Moreover, the coupling of laser ablation systems to MC-ICP-MS instruments has resulted in the ability to acquire accurate and precise isotopic ratios for many elements at high spatial resolution (hundreds of microns or less).<sup>3–6</sup> Recent advances have also been achieved in U–Pb geochronological studies of accessory minerals by laser ablation-MC-ICP-MS<sup>7</sup> despite the fact that many physical and

chemical principles involved in the laser ablation process are still not well understood.<sup>2</sup> Although the U–Pb dates obtained by LA-MC-ICP-MS are less precise<sup>7</sup> (typical  $2\sigma$  error on  $^{207}\text{Pb}/^{206}\text{Pb}$  age  $\sim 1\%$ ) compared with ID-TIMS analyses, this method has certain advantages when employed for certain research projects. For example, a provenance study based on obtaining ID-TIMS age determinations for a large detrital zircon population ( $\sim 100$ )<sup>8–10</sup> would result in an extremely arduous and labour intensive investigation requiring weeks (or months) of instrument time.

In this study, we report U–Pb age determinations for zircons obtained using a MC-ICP-MS coupled to a frequency quintupled ( $\lambda = 213$  nm) Nd:YAG laser ablation system. The MC-ICP-MS instrument at the University of Alberta has been fitted with a modified collector block containing 12 Faraday collectors and three ion counting detectors dispersed on the low mass side of the array (Table 1). The accuracy and precision of the analytical protocols employed during this study are demonstrated through the dating of well-studied, international zircon standards (*e.g.* Fig. 1), and investigation of a detrital zircon population previously investigated by ID-TIMS and SHRIMP.

## 2. Experimental

### 2.1. Instrumentation—multiple ion counting system

Data were acquired using a Nu Plasma MC-ICP-MS (Nu Instruments, UK) coupled to a frequency quintupled ( $\lambda = 213$  nm) Nd:YAG laser ablation system (New Wave Research, USA). The collector configuration allows for the simultaneous acquisition of ion signals ranging from mass  $^{238}\text{U}$  to  $^{203}\text{Tl}$ , an important factor in obtaining highly precise and accurate

**Table 1** Configuration of the 'U–Pb collector block' used for laser ablation experiments<sup>a</sup>

EX-H	H6	H5	H4	H3	H2	H1	AX	L1	L2	IC0	IC1	L3	IC2	EX-L	
Far. <sup>238</sup> U	Far. <sup>235</sup> U	Far.	Far.	Far.	Far.	Far.	Far.	Far.	Far.	Far.	<sup>207</sup> Pb	<sup>206</sup> Pb <sup>204</sup> Hg	Far. <sup>205</sup> Tl	<sup>204</sup> Pb <sup>204</sup> Hg <sup>202</sup> Hg	Far. <sup>203</sup> Tl

<sup>a</sup> The first acquisition sequence is used during the 30 seconds laser ablation analysis of the sample (Tl and non-Tl-doped runs). The second sequence measures the baseline counts and those recorded during ablation (integrations of 5 seconds each) of <sup>202</sup>Hg and <sup>204</sup>Hg for the non-Tl doped experiments.

U–Pb age determinations (Table 1; Fig. 2). <sup>207</sup>Pb, <sup>206</sup>Pb, and <sup>204</sup>Pb (+<sup>204</sup>Hg) signals are measured on the ion counting channels, whereas U and Tl isotopes are acquired on Faraday collectors. Voltages across the quadrupole lenses are optimized so as to ensure coincidence and flat-topped peak shapes (Fig. 2). The ion counters consist of discrete dynode multipliers (manufactured by ETP) and ion signals are bent into the electron multiplier entrances using small deflectors. The latter offer a simple, but effective, means of protecting the ion counters from excessive beams (typically > 10<sup>7</sup> cps; counts per second) that may be incident on the devices. The multipliers can safely measure signals up to several (1–2) × 10<sup>6</sup> cps; however, ion signals were kept below 1 × 10<sup>6</sup> cps in almost all of the laser ablation analyses of zircon so as to prolong the longevity of the detectors. The linearity and stability of the ion counters are better than 0.2% during any one analytical session, whereas dark noise is 0.1 cps or better. A more detailed description of the ion counting system and that for the NuPlasma instrument is featured on the Nu Instruments web site: <http://www.nu-ins.com/products.html>.<sup>11</sup> In this configuration it is not possible to measure simultaneously the <sup>208</sup>Pb ion signal. The instrument settings for both the laser system and MC-ICP-MS used in this study are listed in Table 2.

## 2.2. Ion counter calibration and linearity

The Faraday-ion counter factor is determined using a mixed 0.4 ppb standard solution of Pb (NIST SRM 981 standard) and Tl (NIST SRM 997 standard). The Faraday-multiplier calibration is calculated using a two sequence acquisition, where the <sup>207</sup>Pb/<sup>206</sup>Pb (= 0.914 585)<sup>12</sup> is measured on the IC1 (ion

counter #1)–L3 (Faraday) combination. The IC0 (ion counter #0) and IC2 (ion counter #2) calibrations are determined against the IC1 bias using the measured <sup>207</sup>Pb/<sup>206</sup>Pb and <sup>206</sup>Pb/<sup>204</sup>Pb (= 16.9356)<sup>12</sup> values, respectively. This approach is similar to that adopted in previous isotopic studies involving MC-ICP-MS instruments equipped with multiple ion-counting devices.<sup>13</sup> Over a ~ 10 hour period, the multiplier biases varied between 0.2 and 0.5%. The long-term stability of the ion-counter biases is monitored on a monthly basis, and corrections are applied to multiplier voltages so as to ensure that the relative efficiencies of the three ion counters remain between ~ 80 and 90%.

The linearity of the multiple ion counting system is demonstrated through a series of ablation experiments on a single grain of the in-house (Proterozoic) zircon standard LH94-15 (described below). The grain was ablated (for 30 s) at variable laser power outputs so as to vary the total Pb (or <sup>206</sup>Pb) count rate from ~ 40 000 to > 800 000 cps (Fig. 3A). The results indicate that regardless of the total number of cps, the common Pb corrected <sup>207</sup>Pb/<sup>206</sup>Pb values are identical and yield an external (2σ) reproducibility of approximately 0.2%. The optimal range for the Pb ion signal measured on the ion counters, however, should be governed by the desired level of internal precision; as shown in Fig. 3A the large internal errors for the first two runs are simply a reflection of their lower total Pb count rates. The co-linearity of the IC0 (measures <sup>207</sup>Pb) and IC1 (measures <sup>206</sup>Pb) ion detectors is further illustrated in Fig. 3B, and was evaluated by measuring their respective efficiencies by using a series of NIST SRM 981–Tl (NIST SRM 997)-doped solutions (0.5 ppb to ~ 0.05 ppb), yielding variable Pb ion signal intensities from 0.1 to 1.0 × 10<sup>6</sup> cps of <sup>206</sup>Pb. The relative efficiencies are positively correlated to the absolute Pb ion signal, and define a well-correlated linear regression ( $r^2 = 0.991$ ).

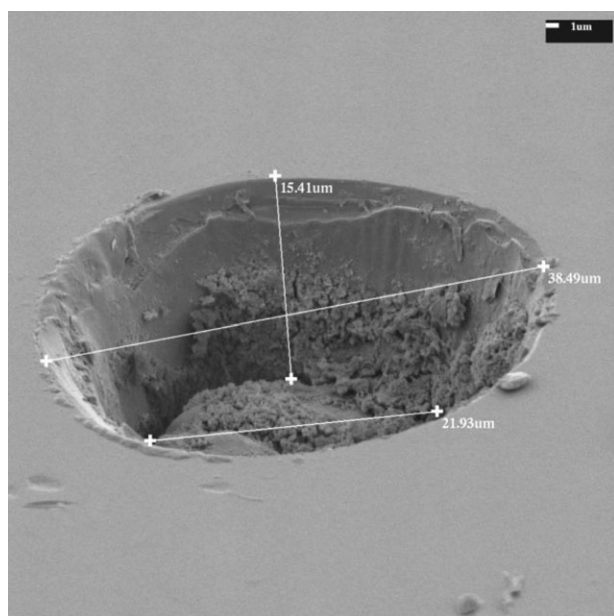


**Fig. 1** Scanning electron microscope photograph of a laser ablation pit within the fragment of international zircon standard BR266. The pit is approximately 40 μm wide and 15 μm deep. Note the absence of welding surrounding the perimeter of the crater.

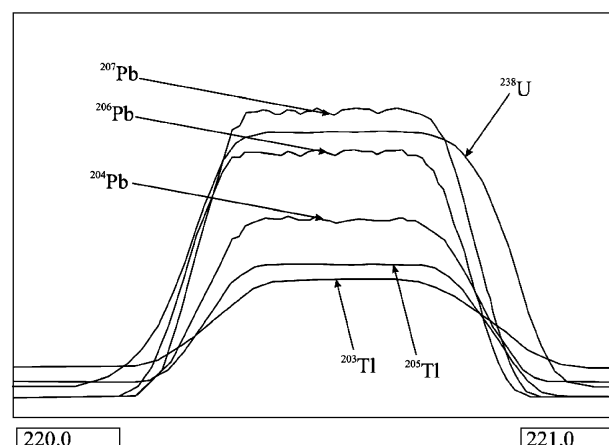


**Fig. 2** Typical beam profiles obtained with the multiple ion counter collector configuration employed in this study. Ion signals result from the aspiration of a mixed natural uranium–NBS 981 (Pb)–NBS 997 (Tl) solution yielding the following intensities: <sup>238</sup>U ~ 100 mV on Faraday (EX-H); <sup>207</sup>Pb ~ 400 000 cps on IC0; <sup>206</sup>Pb ~ 450 000 cps on IC1; <sup>205</sup>Tl ~ 25 mV on Faraday (L3); <sup>204</sup>Pb ~ 27 000 on IC2; <sup>203</sup>Tl ~ 10 mV on Faraday (EX-L). In order to achieve the alignment, the axial reference mass is 220.6.

**Table 2** Operating conditions and instrument settings

ICP		Laser	
MC-ICP-MS			
Model	Nu plasma from Nu Instruments	Model	UP213 Nd:YAG—New Wave Research with aperture imaging system
Forward power	1300 W	Wavelength	213 nm
Reflected power	≤ 10 W	Max. output energy	3 mJ per pulse @ 20 Hz using a 160 μm spot size
Cool gas flow rate	13 L min <sup>-1</sup> (Ar)	Pulse width	3 ns
Auxiliary gas flow rate	1 L min <sup>-1</sup> (Ar)	Energy density	2–3 J cm <sup>-2</sup>
Sample transport:		Focus	Fixed at sample surface
Ablation cell	1 L min <sup>-1</sup> (He)	Repetition rate	Variable from 1 to 20 Hz
DSN-100	Membrane—3.00 to 3.50 L min <sup>-1</sup> (Ar) heated to 110 °C Spray chamber—0.30 L min <sup>-1</sup> (Ar) heated to 110 °C	Spot size	Single spot analysis ≤ 40 μm
Nebuliser-DSN.	Glass Expansion micromist (borosilicate glass)—100 μL min <sup>-1</sup> equipped with Teflon PTFE adaptor and PFA Teflon tubing (1.3 mm od × 0.25 mm id)		
Sampler cone	Ni with 1.15 mm orifice		
Skimmer cone	Ni with 0.6 mm orifice		

### 2.3. Measurement systematics

A routine laser ablation U–Pb analysis consists of a 30 s blank measurement prior to the start of ablation, which includes measurement of the <sup>204</sup>Hg contribution (typically ~ 700 to 1000 cps) measured on IC2. Prior to the start of a Tl-doped ablation run, a ~ 1 ppb solution of Tl is aspirated into the ICP source using a DSN-100 desolvating introduction system (Nu Instruments). The measured <sup>205</sup>Tl/<sup>203</sup>Tl value is used to correct the measured Pb isotope ratios for instrumental mass bias using the reference value of 2.3871.<sup>14</sup> There has been some

debate over the last decade with regard to which study (using either Tl-doping, double- or triple-Pb spike techniques) yields the most accurate values for the NIST SRM 981 Pb standard.<sup>15–17</sup> The relative deviations reported by these individual studies are at the 100s of ppm level, and are therefore insignificant with respect to the accuracies obtained in this study since these are at the percent level (*i.e.*, several orders of magnitude larger). Moreover, recent laser ablation U–Pb studies using both quadrupole<sup>18,19</sup> and MC-ICP-MS<sup>7</sup> instrumentation clearly indicate that Tl ± U ± Np ± Bi doping effectively corrects for instrumental mass bias.

Ablated particles are transported in a He carrier gas and mixed with nebulized thallium *via* a Y-connection located just prior to the torch box. The use of He as the carrier gas reduces the degree of Pb–U within-run fractionation during single spot ablation analyses,<sup>20</sup> and typically results in increased sensitivity.<sup>1,21</sup> Moreover, the solenoid valves normally used to control the gas flow into and out of the ablation cell were not utilized so as to avoid possible cross contamination of ablated particles between standards and unknowns; the sample-out line (Saint-Gobain Tygon<sup>®</sup> tubing) from the laser ablation cell was fed directly to the Y-connection. All ablation experiments were conducted using relatively low energy densities (between 2 and 3 J cm<sup>-2</sup>) so as to limit the <sup>206</sup>Pb ion signals to < 1 × 10<sup>6</sup> cps. The <sup>206</sup>Pb/<sup>238</sup>U measured values are positively correlated with the DSN membrane (Ar) gas flow rate (usually 3.00–3.50 L min<sup>-1</sup>). This is an expected result since varying the mixture of He *versus* Ar within the sample-out tube will most certainly change the plasma characteristics.<sup>1,21</sup>

Correction for instrumental drift during a single laser ablation session of unknown zircons using the Tl-doping method was achieved by a ‘standard–sample–standard’ bracketing technique; this typically involved analysis of the internal standard (LH94-15) after every 10–12 unknown zircon grains.

In recent LA-ICP-MS U–Pb studies,<sup>2,22</sup> the Tl-doping protocol was abandoned in favor of direct ‘standard–sample’ normalization using well-characterized international zircon standards such as 91500. The main concern of these investigations once again centered on the ‘inadequate’ correction of the instrumental mass bias for Pb using Tl during laser ablation experiments (as discussed earlier). However, in order to compensate for the lack of an instantaneous mass bias correction (as is the case for Tl-doped ablation runs), the bracketing of unknown zircon grains requires a significantly more elaborate

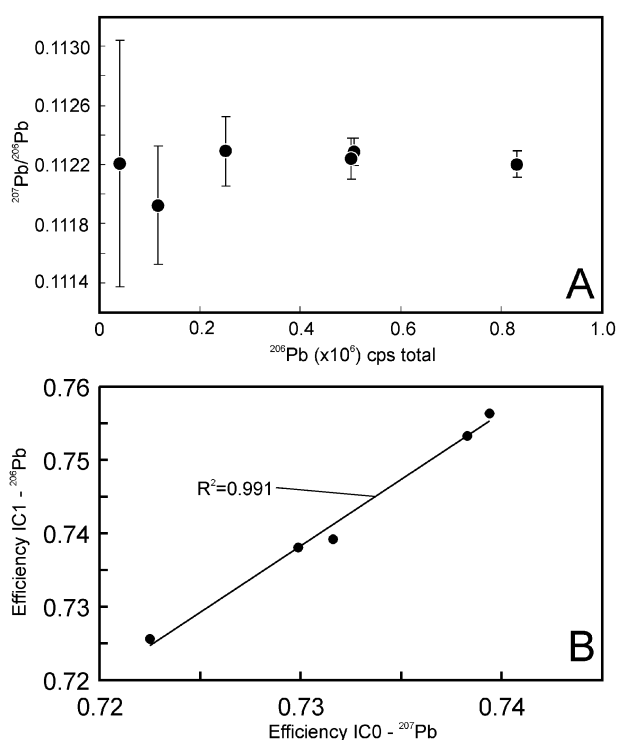


**Fig. 3** Plot of (A) common Pb corrected <sup>207</sup>Pb/<sup>206</sup>Pb versus total <sup>206</sup>Pb count rate (counts per second). Laser output power was varied in order to obtain a variable total Pb count rate using the same LH94-15 zircon fragment. (B) Co-linearity of IC0 and IC1 ion detectors measured with a series of NIST SRM 981–Tl (NIST SRM 997)-doped solutions. Error bars are at the 2σ level.

normalization procedure involving the use of several well-characterized zircon standards (*e.g.*, ref. 22). Thus, one important consequence of the matrix-matched protocol is the increased instrument time (and related increase in cost) required to analyze the same number of unknown grains compared with the TI-doped technique. This feature may be of significant importance in the U–Pb dating of detrital zircon populations since a significant minimum number ( $n > 50$ ) of grains are required for meaningful provenance studies. For example, it took at least 30% more time to obtain an identical number of analyses for BR266 (Table 3) using the non-TI-doping method compared with the TI-doping protocol. Despite this feature, a comparative investigation of both analytical protocols was conducted using international zircon standards BR266 and 91500 in order to determine their feasibility with regard to the analysis of detrital zircon populations.

#### 2.4. Zircon and glass standards

The accuracy and precision of the analytical protocol described in this study were validated using well-established international zircon standards BR266<sup>23,24</sup> and 91500,<sup>22,25</sup> zircon from sam-

ple LH-94-15 previously dated by ID-TIMS,<sup>26</sup> and the international SRM NIST 612 glass wafer (Table 4). Despite its glass matrix, previous laser ablation-ICP-MS and SHRIMP U–Pb dating studies have extensively used the SRM NIST 610 and 612 glass wafers for evaluating the effect of various instrument parameters (*e.g.*, spot size) on inter-element fractionation.<sup>1,18,23</sup>

The fragment of standard BR266 used in this study was obtained from A. Kennedy (Curtin University, Perth), and originates from a Sri Lankan centimeter-sized gem-quality zircon. The majority of gem quality zircons from Sri Lanka are believed to have formed in late-stage pegmatites found in the metamorphic rocks of the Highland Group.<sup>27,28</sup> Stern and Amelin,<sup>24</sup> recently reported 22 new (high precision) ID-TIMS U–Pb dates for randomly selected fragments of BR266, which yielded weighted mean <sup>206</sup>Pb/<sup>238</sup>U and <sup>207</sup>Pb/<sup>206</sup>Pb ages of  $559.0 \pm 0.2$  Ma and  $562.6 \pm 0.2$  Ma, respectively.

Zircon standard 91500 was originally isolated from a porphyroblastic syenite gneiss that is cross-cut by sheets or sills of syenite pegmatite, Renfrew County, Ontario.<sup>25</sup> For this study, fragments of 91500 were purchased from the SARM (Service d'Analyse des Roches et des Minéraux) laboratory of the CRPG (Centre de Recherches Pétrographiques et Géochi-

**Table 3** Laser ablation results and ID-TIMS reference values for BR266 international zircon standard

	<sup>204</sup> Pb cps	<sup>206</sup> Pb cps rad.	<sup>206</sup> Pb/ <sup>204</sup> Pb	<sup>207</sup> Pb/ <sup>206</sup> Pb	Error (2σ)	<sup>207</sup> Pb/ <sup>235</sup> U	Error (2σ)	<sup>206</sup> Pb/ <sup>238</sup> U	Error (2σ)	<sup>206</sup> Pb/ <sup>238</sup> Pb age (Ma)	Error (2σ)
BR266 ID-TIMS				0.058 88	0.000 005	0.7354	0.0002	0.090 58	0.000 02	559.0	0.3
Non-TI-doped											
1	0	429 950	Infinite	0.0597	0.0003	0.7465	0.0106	0.0916	0.0020	565	12
2	0	437 923	Infinite	0.0596	0.0003	0.7409	0.0105	0.0911	0.0018	562	11
3	0	442 719	Infinite	0.0597	0.0003	0.7416	0.0105	0.0911	0.0019	562	12
4	0	449 380	Infinite	0.0597	0.0003	0.7500	0.0106	0.0921	0.0018	568	11
5	0	448 268	Infinite	0.0597	0.0003	0.7461	0.0105	0.0916	0.0016	565	10
6	0	449 533	Infinite	0.0597	0.0003	0.7366	0.0104	0.0904	0.0017	558	10
7	0	448 890	Infinite	0.0598	0.0003	0.7518	0.0106	0.0922	0.0018	569	11
8	0	466 749	Infinite	0.0598	0.0003	0.7531	0.0106	0.0923	0.0016	569	10
9	0	464 539	Infinite	0.0599	0.0003	0.7421	0.0105	0.0908	0.0017	560	11
10	0	458 280	Infinite	0.0598	0.0003	0.7425	0.0105	0.0911	0.0018	562	11
11	0	444 659	Infinite	0.0597	0.0003	0.7489	0.0105	0.0920	0.0017	567	10
12	0	454 989	Infinite	0.0597	0.0003	0.7475	0.0105	0.0918	0.0016	566	10
13	0	453 721	Infinite	0.0600	0.0003	0.7430	0.0105	0.0908	0.0018	560	11
14	0	457 346	Infinite	0.0599	0.0003	0.7519	0.0106	0.0921	0.0017	568	10
15	0	453 693	Infinite	0.0598	0.0003	0.7517	0.0106	0.0921	0.0017	568	11
Average=				0.05979		0.7463		0.09153		565	
STD (2σ)				0.00020		0.0099		0.00122		7	
STD (%)				0.34		1.33		1.33			
TI-doped											
1	0	317 491	Infinite	0.059 19	0.0004	0.7627	0.019	0.09 337	0.0026	575	16
2	0	315 599	Infinite	0.058 65	0.0004	0.7450	0.019	0.092 07	0.0026	568	16
3	0	322 428	Infinite	0.058 83	0.0004	0.7573	0.019	0.093 28	0.0025	575	16
4	0	336 899	Infinite	0.059 01	0.0004	0.7477	0.019	0.091 84	0.0025	566	16
5	27	331 866	12 291	0.058 77	0.0004	0.7397	0.019	0.091 28	0.0024	563	15
6	23	349 802	15 209	0.058 77	0.0005	0.7611	0.019	0.093 90	0.0025	579	15
7	0	329 793	Infinite	0.059 00	0.0004	0.7533	0.019	0.092 53	0.0027	571	17
8	0	332 186	Infinite	0.058 71	0.0004	0.7492	0.019	0.092 50	0.0026	570	16
9	0	329 255	Infinite	0.058 91	0.0004	0.7472	0.019	0.091 93	0.0024	567	15
10	0	328 537	Infinite	0.058 70	0.0003	0.7431	0.019	0.091 74	0.0026	566	16
11	0	320 908	Infinite	0.058 76	0.0004	0.7488	0.019	0.092 47	0.0027	570	16
12	0	338 788	Infinite	0.058 85	0.0005	0.7467	0.019	0.091 95	0.0026	567	16
13	0	333 996	Infinite	0.058 69	0.0004	0.7331	0.018	0.090 53	0.0024	559	15
14	13	341 289	26 253	0.058 79	0.0004	0.7336	0.018	0.090 39	0.0024	558	15
15	9	328 805	36 534	0.058 78	0.0004	0.7356	0.019	0.090 71	0.0025	560	15
Average=				0.0588		0.7469		0.0920		568	
STD (2σ)				0.0003		0.0183		0.0021		12	
STD (%)				0.50		2.45		2.24			

**Table 4** Laser ablation analyses of SRM NIST 612 glass

Analysis #	$^{207}\text{Pb}/^{206}\text{Pb}$	Error ( $2\sigma$ )	$^{207}\text{Pb}/^{235}\text{U}$	Error ( $2\sigma$ )	$^{206}\text{Pb}/^{238}\text{U}$	Error ( $2\sigma$ )
1	0.9073	0.006	36.538	0.304	0.2923	0.004
2	0.9075	0.002	36.117	0.408	0.2889	0.006
3	0.9122	0.006	36.221	0.584	0.2883	0.006
4	0.9099	0.006	36.662	0.584	0.2926	0.006
5	0.9148	0.004	35.777	0.574	0.2838	0.006
6	0.9098	0.004	36.961	0.318	0.2948	0.004
7	0.9032	0.004	37.422	0.412	0.3009	0.004
8	0.9041	0.004	37.005	0.436	0.2970	0.004
9	0.9015	0.004	36.729	0.432	0.2959	0.004
10	0.9083	0.006	37.373	0.434	0.2987	0.006
11	0.9064	0.004	36.542	0.498	0.2926	0.006
12	0.9047	0.006	36.507	0.786	0.2930	0.008
13	0.9025	0.004	36.438	0.656	0.2931	0.006
14	0.9117	0.004	37.114	0.570	0.2954	0.006
Average	0.9074		36.6719		0.2934	
STD ( $2\sigma$ )	0.0079		0.9407		0.0088	
STD (%)	0.88		2.57		2.99	
True value	0.90734 <sup>a</sup>		34.6481 <sup>b</sup>		0.28186 <sup>b</sup>	

<sup>a</sup>  $^{207}\text{Pb}/^{206}\text{Pb}$  value calculated using  $^{207}\text{Pb}/^{204}\text{Pb}$  and  $^{206}\text{Pb}/^{204}\text{Pb}$  values determined by double-spike ID-TIMS (Woodhead and Hergt<sup>33</sup>); <sup>b</sup>  $^{206}\text{Pb}/^{238}\text{U}$  and  $^{207}\text{Pb}/^{235}\text{U}$  values calculated using common Pb isotope values determined by double-spike ID-TIMS (Woodhead and Hergt<sup>33</sup>) and the natural  $^{238}\text{U}/^{235}\text{U} = 137.88$ .<sup>31</sup>

miques; Nancy, France). The mean ( $n = 11$  fragments) ID-TIMS weighted average  $^{207}\text{Pb}/^{206}\text{Pb}$  age reported by Wiedenbeck *et al.*<sup>25</sup> is  $1065.4 \pm 0.3$  Ma.

The in-house zircon standard consists of clear, inclusion-free grains taken from two of three zircon fractions from sample LH94-15, a homogeneous calc-alkaline enderbite, which yielded a concordant ID-TIMS age of  $1830 \pm 1$  Ma (the average atomic ratios for three previously published near-concordant to concordant analyses are given in Table 5).<sup>26</sup> The crystal morphology of the zircons implies an igneous derivation, and thus the age is interpreted as a crystallization age of the calc-alkaline body.<sup>26</sup> LH94-15 zircons typically contain Pb and U contents of  $\sim 100$  and  $\sim 300$  ppm, respectively, and during ablation runs normally yield  $\sim 300\,000$  to  $\sim 800\,000$  cps of  $^{206}\text{Pb}$  when using a  $40\ \mu\text{m}$  spot size.

### 3. Results and discussion

#### 3.1. Common Pb correction and error propagation

Horstwood *et al.*<sup>7</sup> have clearly demonstrated the importance of performing a common Pb correction in the U–Pb dating of accessory minerals (*e.g.*, monazite) when using laser ablation MC-ICP-MS instrumentation. A correction may prove important in studies of detrital zircon populations in order to avoid analysis bias.<sup>7</sup> The instrument configuration employed in this study allows for the accurate measurement of small ion signals at mass 204 ( $^{204}\text{Pb} + ^{204}\text{Hg}$ ), and a common Pb correction can be readily applied regardless of the mineral being dated. Thus, a detailed evaluation of the mass 204 ion signal detected on IC2 was conducted for all Tl-doped ablation experiments. In the following section and throughout the manuscript, common Pb corrections involved using the projected age of the mineral and the corresponding initial Pb isotopic compositions taken from the two-stage evolution model of Stacey and Kramers.<sup>29</sup>

Fig. 4 illustrates two examples of the significant correlation between the total 204 ion signal (cps) *versus* the common Pb-corrected (*i.e.* radiogenic)  $^{207}\text{Pb}/^{206}\text{Pb}$  values for individual Tl-doped laser ablation analyses (30 s duration) of international zircon standards BR266 and 91500. Theoretical considerations predict that if the  $^{204}\text{Hg}$  carrier gas corrected 204 ion signal is in fact common Pb originating from the zircon grain being analyzed, then a plot of 204 ion signal *versus* common Pb corrected  $^{207}\text{Pb}/^{206}\text{Pb}$  values should yield a horizontal line.

However, a number of individual analyses produce well-correlated negative, linear regressions (Fig. 4), indicating that there is an excess of ions on mass 204 being detected. Excellent quality zircon crystals devoid of inclusions, fractures or alteration generally contain negligible amounts of indigenous common Pb; thus, the source of excess mass 204 ions is not accurately known but can originate from either  $^{204}\text{Pb}$  ions generated from the epoxy mount and extraneous to the grain being analyzed, or a polyatomic, molecular isobaric interference produced during the ablation process, or additional  $^{204}\text{Hg}$  produced during the ablation process. It is difficult to evaluate the validity of the second option; however, common Pb originating from the epoxy would systematically generate an excess 204 ion signal for all laser ablation analyses. The  $^{204}\text{Pb}$  cps listed in Tables 3 and 5 indicate that this is clearly not the case. Moreover, this explanation is less likely since for every laser ablation analysis care was taken to avoid ablating the surrounding epoxy. With regard to the possible production of additional  $^{204}\text{Hg}$  during ablation runs, a series of experiments were designed in order to measure the  $^{204}\text{Hg}/^{202}\text{Hg}$  value and the total count rates for both  $^{204}\text{Hg}$  and  $^{202}\text{Hg}$  prior and subsequent to the start of several zircon ablation runs. This was accomplished by decreasing the reference mass in the axial Faraday collector by two mass units in order to measure  $^{204}\text{Hg}$  in IC1 and  $^{202}\text{Hg}$  in IC2; the results are listed in Table 6. During the first part of the experiment (over  $\sim 1$  hour), repeated measurements of the Hg isotopic composition and  $^{204}\text{Hg}$  and  $^{202}\text{Hg}$  count rates (efficiency normalized values) of the gas + acid blank were taken. Ablation runs were subsequently conducted using the in-house zircon standard (LH94-15) and five unknown detrital Archean zircons to determine their Hg isotopic composition and Hg count rates. The results listed in Table 6 indicate that statistically there is no clear evidence for the systematic production (or increase) of Hg occurring subsequent to the start of the ablation runs. In fact, the  $^{204}\text{Hg}/^{202}\text{Hg}$  composition of the gas + acid blank and that measured during the ablation of the zircon grains are virtually identical (Table 6); however, these are both lower than the accepted, natural  $^{204}\text{Hg}/^{202}\text{Hg}$  value of 0.229 883,<sup>30</sup> while the measured Hg isotopic compositions listed in Table 6 should be larger than the natural value due to the superimposed effects of instrumental mass bias. Possible causes include the presence of an isobaric interference on mass  $^{202}\text{Hg}$  that is lowering the  $^{204}\text{Hg}/^{202}\text{Hg}$  value, or Hg is undergoing continuous fractional

**Table 5** Laser ablation results and ID-TIMS reference values for 91500 international zircon standard

	$^{204}\text{Pb}/$ cps	$^{206}\text{Pb}/$ cps rad.	$^{206}\text{Pb}/$ $^{204}\text{Pb}$	$^{207}\text{Pb}/$ $^{206}\text{Pb}$	Error ( $2\sigma$ )	$^{207}\text{Pb}/$ $^{235}\text{U}$	Error ( $2\sigma$ )	$^{206}\text{Pb}/$ $^{238}\text{U}$	Error ( $2\sigma$ )	$^{206}\text{Pb}/^{238}\text{Pb}$ age (Ma)	Error ( $2\sigma$ )
91500 ID-TIMS				0.074 88	0.000 01	1.8502	0.0008	0.179 17	0.000 08	1062.4	0.4
Non-Tl-doped											
1	0	53 417	Infinite	0.0760	0.0010	1.7761	0.0534	0.1738	0.0059	1033	35
2	0	53 833	Infinite	0.0762	0.0010	1.8140	0.0545	0.1769	0.0059	1050	35
3	0	54 212	Infinite	0.0769	0.0010	1.8045	0.0542	0.1744	0.0055	1036	33
4	0	52 536	Infinite	0.0772	0.0009	1.7686	0.0531	0.1703	0.0055	1014	32
5	0	53 629	Infinite	0.0771	0.0009	1.8098	0.0544	0.1745	0.0057	1037	34
6	0	53 917	Infinite	0.0769	0.0009	1.8109	0.0544	0.1751	0.0056	1040	33
7	0	55 320	Infinite	0.0771	0.0010	1.7815	0.0535	0.1718	0.0054	1022	32
8	0	56 360	Infinite	0.0769	0.0010	1.7700	0.0532	0.1712	0.0055	1018	32
9	0	54 463	Infinite	0.0766	0.0011	1.8357	0.0552	0.1780	0.0061	1056	36
10	0	57 244	Infinite	0.0763	0.0010	1.8298	0.0550	0.1784	0.0060	1058	35
11	0	60 615	Infinite	0.0765	0.0009	1.8268	0.0549	0.1774	0.0058	1053	35
12	0	61 214	Infinite	0.0770	0.0009	1.8310	0.0550	0.1767	0.0058	1049	34
13	0	57 892	Infinite	0.0774	0.0013	1.8505	0.0556	0.1779	0.0060	1056	35
14	0	59 194	Infinite	0.0766	0.0010	1.8377	0.0552	0.1784	0.0058	1058	34
15	0	59 436	Infinite	0.0768	0.0009	1.8088	0.0544	0.1751	0.0059	1040	35
16	0	59 158	Infinite	0.0767	0.0009	1.8285	0.0549	0.1772	0.0058	1052	35
17	0	58 785	Infinite	0.0767	0.0009	1.8348	0.0551	0.1778	0.0059	1055	35
18	0	60 038	Infinite	0.0772	0.0010	1.8189	0.0546	0.1752	0.0057	1041	34
Average=				0.0768		1.8132		0.1756		1043	
STD ( $2\sigma$ )				0.0008		0.0494		0.0051		28	
STD (%)				0.98		2.72		2.90			
Tl-doped											
1	0	59 706	Infinite	0.0743	0.0010	1.8134	0.0546	0.1770	0.0064	1050	38
2	0	59 448	Infinite	0.0745	0.0009	1.7836	0.0536	0.1736	0.0059	1032	35
3	0	60 463	Infinite	0.0748	0.0009	1.7846	0.0536	0.1732	0.0058	1030	35
4	0	59 347	Infinite	0.0749	0.0009	1.8071	0.0543	0.1751	0.0059	1040	35
5	10	60 531	6053	0.0747	0.0011	1.8433	0.0554	0.1789	0.0062	1061	37
6	0	62 494	Infinite	0.0755	0.0009	1.8482	0.0555	0.1776	0.0059	1054	35
7	0	62 096	Infinite	0.0747	0.0009	1.8046	0.0542	0.1753	0.0059	1041	35
8	0	64 671	Infinite	0.0754	0.0009	1.8436	0.0554	0.1773	0.0059	1052	35
9	0	65 234	Infinite	0.0751	0.0009	1.8375	0.0552	0.1775	0.0060	1053	36
10	0	64 193	Infinite	0.0752	0.0009	1.8521	0.0557	0.1786	0.0059	1059	35
11	0	66 900	Infinite	0.0761	0.0009	1.8566	0.0558	0.1770	0.0059	1050	35
12	0	65 478	Infinite	0.0752	0.0009	1.8122	0.0545	0.1747	0.0058	1038	34
13	0	58 202	Infinite	0.0749	0.0009	1.8490	0.0556	0.1791	0.0061	1062	36
14	0	60 591	Infinite	0.0755	0.0010	1.8389	0.0553	0.1766	0.0061	1048	36
15	0	62 923	Infinite	0.0755	0.0010	1.8633	0.0560	0.1791	0.0060	1062	35
16	0	64 215	Infinite	0.0751	0.0009	1.8237	0.0548	0.1761	0.0061	1046	36
17	0	62 563	Infinite	0.0748	0.0009	1.8264	0.0549	0.1772	0.0060	1051	36
18	0	68 113	Infinite	0.0749	0.0009	1.8369	0.0552	0.1779	0.0059	1056	35
19	0	62 360	Infinite	0.0746	0.0009	1.8273	0.0549	0.1777	0.0062	1054	37
Average=				0.0750		1.8291		0.1768		1049	
STD ( $2\sigma$ )				0.0009		0.0461		0.0035		19	
STD (%)				1.15		2.52		1.97			

distillation within the plasma. It is difficult to speculate further on the exact origin of the discrepancy between the measured and accepted  $^{204}\text{Hg}/^{202}\text{Hg}$  value since the former has not been reported in any previous study of a similar nature. Thus, the results obtained here indicate that some caution should be exercised in future studies advocating the correction of 'Hg' produced during the laser ablation of zircons.

A mathematical approach was developed for the Tl-doped ablation runs in order to evaluate and correct for the excess ion signal on mass 204. As previously stated, the linear regressions displayed in Fig. 4A and 4C should be horizontal lines, with the Y-intercept equating to the Tl (mass bias)-corrected  $^{207}\text{Pb}/^{206}\text{Pb}$  value determined at the end of the ablation run. The overcorrection can also be displayed by plotting the common Pb corrected  $^{207}\text{Pb}/^{206}\text{Pb}$  values versus the more familiar  $^{206}\text{Pb}/^{204}\text{Pb}$  parameter (Fig. 4B and 4D). For ablation runs with an excess mass 204 ion signal, the Y-intercept ( $^{207}\text{Pb}/^{206}\text{Pb}$  value) is as expected always larger than the Tl-corrected  $^{207}\text{Pb}/^{206}\text{Pb}$

value obtained for the analysis. In contrast, grains not requiring a common Pb correction typically lack a significant correlation (Fig. 4E), and/or yield Y-intercept values that are lower than the Tl-corrected  $^{207}\text{Pb}/^{206}\text{Pb}$ . Based on the results obtained for the NIST 612 glass wafer (Table 4), the Tl-doping mass bias correction employed here yields accurate  $^{207}\text{Pb}/^{206}\text{Pb}$  values. Therefore, a significant difference between the Tl-corrected  $^{207}\text{Pb}/^{206}\text{Pb}$  value for the zircon standards and their accepted  $^{207}\text{Pb}/^{206}\text{Pb}$  ratios is directly attributable to the presence of common Pb. In order to obtain the accurate amount of  $^{204}\text{Pb}$  intrinsic to the zircon standards (BR266, 91500 and LH94-15) and our analytical protocol, the equation generated by the linear regression is equated to the accepted ID-TIMS ages; this in-turn yields the accurate amount of  $^{204}\text{Pb}$ . For zircon grains of unknown age, the linear regression is equated to the Tl-mass bias corrected  $^{207}\text{Pb}/^{206}\text{Pb}$  value (once again, correction only applies if the latter is a lower value compared to the Y-intercept).

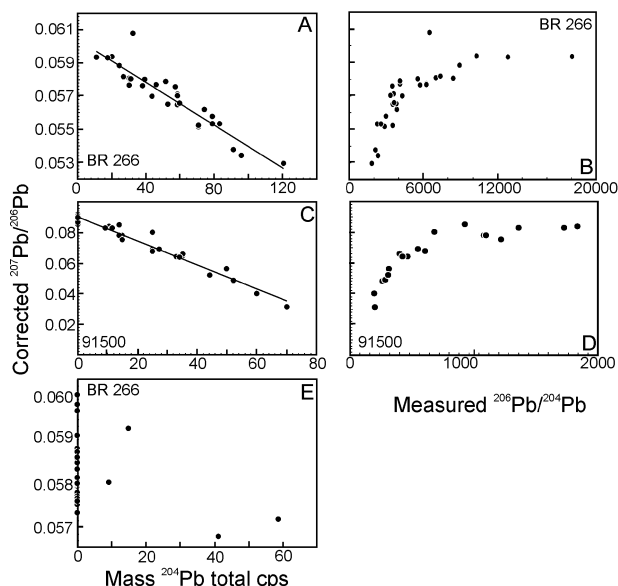


**Fig. 4** Diagrams illustrating the correlation between common Pb corrected  $^{207}\text{Pb}/^{206}\text{Pb}$  values and total mass 204 ion signal for individual TI-doped ablation runs in (A) BR266 and (C) 91500 zircon standard fragments; (B) and (D) plots of corrected  $^{207}\text{Pb}/^{206}\text{Pb}$  values versus measured  $^{206}\text{Pb}/^{204}\text{Pb}$  for fragments BR266 and 91500, respectively. (E) For comparison, a single spot analysis of fragment BR266 not requiring a common Pb correction (analysis #5, Table 5).

For the matrix-matched (non-TI-doped) analyses, the amount of  $^{204}\text{Pb}$  versus  $^{204}\text{Hg}$  (if present) was evaluated with an additional acquisition sequence since instrumental mass bias cannot be monitored instantaneously. The reference mass in the axial collector was again decreased by two atomic mass units in order to measure  $^{204}\text{Hg}$  in IC1 and  $^{202}\text{Hg}$  in IC2 (Table 1). Once again,  $^{202}\text{Hg}$  count rates above background levels during ablation runs were highly variable, and no excess mass 204 counts were detected (Tables 3 and 5).

The analytical uncertainties (= standard deviation/ $\sqrt{n-1}$ ;  $n$  = number of 1 second integrations) associated with  $^{207}\text{Pb}/^{206}\text{Pb}$  and  $^{206}\text{Pb}/^{238}\text{U}$  for individual (single grain) analyses were propagated relative to the external reproducibility (*i.e.*, relative standard deviation = average value/standard deviation at  $2\sigma$  level) obtained for the in-house zircon standard and followed the procedure described in Horstwood *et al.*<sup>7</sup> The measured  $^{207}\text{Pb}/^{235}\text{U}$  values for individual analyses are much less accurate due to the very small  $^{235}\text{U}$  ion signals recorded in most zircons. Therefore, the  $^{207}\text{Pb}/^{235}\text{U}$  value is calculated using the  $^{207}\text{Pb}/^{206}\text{Pb}$  and  $^{206}\text{Pb}/^{238}\text{U}$  (mass bias and blank corrected) values and the natural  $^{238}\text{U}/^{235}\text{U}$  value of 137.88;<sup>31</sup> the identical calculation for the  $^{207}\text{Pb}/^{235}\text{U}$  parameter was adopted by Horstwood *et al.*<sup>7</sup> The associated uncertainties were propagated in the same manner as those outlined for the  $^{207}\text{Pb}/^{206}\text{Pb}$  and  $^{206}\text{Pb}/^{238}\text{U}$  values. Of interest, for zircons with abundant concentrations of U (*e.g.*, LH94-15 with  $\sim 300$  ppm; BR266 with  $\sim 900$  ppm), the measured  $^{207}\text{Pb}/^{235}\text{U}$  and recalculated  $^{207}\text{Pb}/^{235}\text{U}$  values are usually indistinguishable (within analytical uncertainty). The correlation coefficients ( $\rho$  values) for the  $^{207}\text{Pb}/^{235}\text{U}$  and  $^{206}\text{Pb}/^{238}\text{U}$  values were calculated according to the equations defined in Ludwig.<sup>32</sup>

### 3.2. NIST 612 glass and zircon standards

The SRM NIST 612 wafer was ablated using identical laser and MC-ICP-MS settings (Table 2) to those used for the BR266, 91500, internal (LH94-15) zircon standards, and unknown zircons since it contains Pb ( $38.57 \pm 0.2$  ppm) and U ( $37.38 \pm 0.08$  ppm) concentrations comparable to that of an 'average' zircon. The data listed in Table 4 indicate that the TI-

**Table 6** Isotopic composition and count rates of Hg for gas blank and zircon ablation runs

Gas blank:	$^{204}\text{Hg}/^{202}\text{Hg}$	Error ( $2\sigma$ )	$^{204}\text{Hg}$ /cps	Error ( $2\sigma$ )	$^{202}\text{Hg}$ /cps	Error ( $2\sigma$ )
1	0.2132	0.002	1363	16	6381	66
2	0.2178	0.002	1338	14	6145	60
3	0.2107	0.002	1420	16	6749	44
4	0.2124	0.002	1232	20	5813	54
5	0.2108	0.002	1258	14	5980	46
6	0.2132	0.002	1322	20	6209	86
7	0.2127	0.002	1317	20	6188	68
8	0.2145	0.002	1301	14	6068	60
9	0.2162	0.002	1304	22	6044	46
10	0.2122	0.002	1280	20	6053	98
Average	0.2134		1314		6163	
STD ( $2\sigma$ )	0.0045		53		510	
LH94-15:						
Grain-1	0.2122	0.002	1220	20	5747	58
Grain-1	0.2121	0.002	1408	16	6587	92
Grain-2	0.2132	0.002	1467	24	6907	64
Grain-3	0.2112	0.002	1448	14	6872	48
Grain-4	0.2129	0.002	1398	18	6612	58
Average	0.2123		1388		6545	
STD ( $2\sigma$ )	0.0015		196		939	
Archean zircons						
Grain-1	0.2245	0.004	1566	20	6929	72
Grain-2	0.2134	0.002	1334	16	6247	54
Grain-3	0.2127	0.002	1329	16	6239	54
Grain-4	0.2146	0.002	1349	20	6334	48
Grain-5	0.2140	0.002	1369	22	6413	108
Average=	0.2158		1389		6432	
STD ( $2\sigma$ )	0.0098		200		573	

doping method employed during the ablation of the NIST 612 wafer yield an average  $^{207}\text{Pb}/^{206}\text{Pb}$  value ( $0.9074 \pm 0.0079$ ) indistinguishable from the highly precise value of 0.90734 obtained by double-spike TIMS analysis (Table 4).<sup>33</sup> The relative standard deviation ( $2\sigma$ ) of the  $^{206}\text{Pb}/^{238}\text{U}$  and  $^{207}\text{Pb}/^{206}\text{Pb}$  values are approximately 3% and 0.9%, respectively (Table 4). Similar or lower external reproducibility was achieved during an individual analytical session for the TI-doped ablation analyses of BR266 (Table 3) and 91500 (Table 5) zircon standards.

Laser ablation analyses of BR266 in this study using a 40  $\mu\text{m}$  spot for both matrix-matched and TI-doped analyses are listed in Table 3. Both sets of analyses were collected during two analytical sessions three days apart, and the number of analyses correspond to those measured in  $\sim 2$  (TI-doped) to 2.5 (non-TI-doped) hours. For the non-TI-doped analyses, correction for instrumental mass bias and instrumental drift was achieved with the use of the 91500 zircon standard ablated at the same conditions. The non-TI doped analyses are concordant and yield a highly precise weighted average  $^{207}\text{Pb}/^{206}\text{Pb}$  age of  $566.6 \pm 1.5$  Ma. This date is only a few million years older than the recommended  $^{207}\text{Pb}/^{206}\text{Pb}$  age of  $562.6 \pm 0.2$  Ma.<sup>24</sup> In addition, the calculated ( $2\sigma$ ) external reproducibility (rsd) is best for the non-TI-doped runs since these are roughly 0.3% for the  $^{207}\text{Pb}/^{206}\text{Pb}$  values and approximately 1.3% for both Pb/U ratios (Table 3). To our knowledge, these uncertainties are amongst the lowest (if not the lowest) reported in the literature for laser ablation U–Pb analysis of zircon. The TI-doped analyses are also concordant and yield a highly precise and accurate weighted average  $^{207}\text{Pb}/^{206}\text{Pb}$  age of  $564.7 \pm 1.9$  Ma, which is indistinguishable from both the non-TI-doped ( $566.6 \pm 1.5$  Ma) and ID-TIMS  $^{207}\text{Pb}/^{206}\text{Pb}$

age of  $562.6 \pm 0.2$  Ma. The associated ( $2\sigma$ ) external reproducibility (rsd) for the Tl-doped analyses are 0.5% for the  $^{207}\text{Pb}/^{206}\text{Pb}$  and 2.2 to 2.5% for the Pb/U values (Table 3). For both the non- and Tl-doped analyses, the amount of  $^{204}\text{Pb}$  is extremely low or non-existent (0 cps; Table 3), which attests to the 'clean' nature of this zircon standard. Overall, the results for BR266 listed in Table 3 are remarkably reproducible and accurate when compared with published ID-TIMS and SHRIMP ages for BR266.

Table 5 reports the laser ablation results for both non-Tl- and Tl-doped analyses obtained using a 40  $\mu\text{m}$  spot size from the same 91500 grain fragment (several hundred microns wide). Both sets of analyses were obtained consecutively on the same day, and correction for instrumental mass bias and instrumental drift was achieved with ablation runs of zircon standard BR266. The non-Tl-doped analyses ( $n = 18$ ) yield a precise date of  $1066 \pm 5.8$  Ma, which is indistinguishable from the ID-TIMS age of  $1065.4 \pm 0.3$  Ma.<sup>25</sup> The calculated ( $2\sigma$ ) external reproducibility (rsd) for the  $^{207}\text{Pb}/^{206}\text{Pb}$ ,  $^{206}\text{Pb}/^{238}\text{U}$  and  $^{206}\text{Pb}/^{235}\text{U}$  values are  $\sim 1\%$ , 2.7% and 2.9%, respectively (Table 5). These values are somewhat higher than those calculated for the non-Tl analyses of BR266 (Table 3), and are directly attributable to the much lower count rates ( $\sim 60\,000$  versus 450 000 cps of  $^{206}\text{Pb}$ ) recorded for the 91500 runs due to the much lower Pb content ( $\sim 15$  ppm)<sup>25</sup> in this standard. The U–Pb ablation results for the Tl-doped analysis are listed in Table 5. These yield a precise weighted average  $^{207}\text{Pb}/^{206}\text{Pb}$  age of  $1069.5 \pm 5.8$  Ma, which is indistinguishable from the recommended ID-TIMS age ( $1065.4 \pm 0.3$  Ma)<sup>25</sup> and the age obtained for the non-Tl doped runs ( $1066.0 \pm 5.8$  Ma). Compared with the calculated ( $2\sigma$ ) external reproducibility (rsd) for the  $^{207}\text{Pb}/^{206}\text{Pb}$ ,  $^{207}\text{Pb}/^{235}\text{U}$  and  $^{206}\text{Pb}/^{238}\text{U}$  values obtained for the non-Tl-doped runs, those for the Tl-doped analyses are similar or slightly lower ( $\sim 1\%$ ,  $\sim 2.5\%$  and  $\sim 2.0\%$ , respectively). For both analytical protocols, the  $^{204}\text{Pb}$  cps recorded were nil with the exception of one Tl-doped analysis (#5, Table 5) which also attests to the relatively 'clean' nature of this international standard. As is the case for the BR266 zircon standard, the results obtained for both analytical protocols using the 91500 zircon standard are similar and yield both highly precise and accurate ages when compared with the well-established ID-TIMS age. However, the ( $2\sigma$ ) rsd for the Pb/U values seem to be much more consistent with the Tl-doped analyses compared with the non-Tl-doped runs, and independent of the absolute Pb count rates (Tables 3 and 5). Thus, the Tl-doping protocol may be better suited for the analysis of large detrital zircon populations since Pb (and U) concentrations are typically extremely variable between individual grains.

Laser ablation Tl-doped runs obtained for grains of LH94-15 on three separate days over a two month period are shown in Fig. 5. Fig. 5A illustrates the data for February 13th, 2004, subsequent to all of the corrections, error propagations and common Pb correction; the analyses are collinear (MSWD = 0.14) and yield an age of  $1830 \pm 7$  Ma, which is indistinguishable from the ID-TIMS age. The results obtained on April 22nd, 2004, for LH94-15 yield a common-Pb corrected age of  $1826 \pm 6$  Ma, once again indistinguishable from the ID-TIMS age (Fig. 5B). A similar result was obtained on April 27th, 2004, when the data corrected for common Pb yielded an age of  $1828 \pm 6$  Ma (Fig. 5C) and again is indistinguishable from the previously reported ID-TIMS age of  $1830 \pm 1$  Ma.<sup>26</sup> Of importance, the LH94-15 age data shown in Fig. 5 is remarkably consistent despite the fact that it was collected over a three-month period by three different analysts.

The ( $2\sigma$ ) rsd of the  $^{207}\text{Pb}/^{206}\text{Pb}$  values for the BR266 analyses listed in Table 3 and that for the LH94-15 analyses shown in Fig. 5 are 0.3–0.7%; these are lower by a factor of  $\sim 3$ –7 compared with those reported for a recent (long-term) LA-ICP-MS zircon dating investigation.<sup>22</sup> Also of importance,

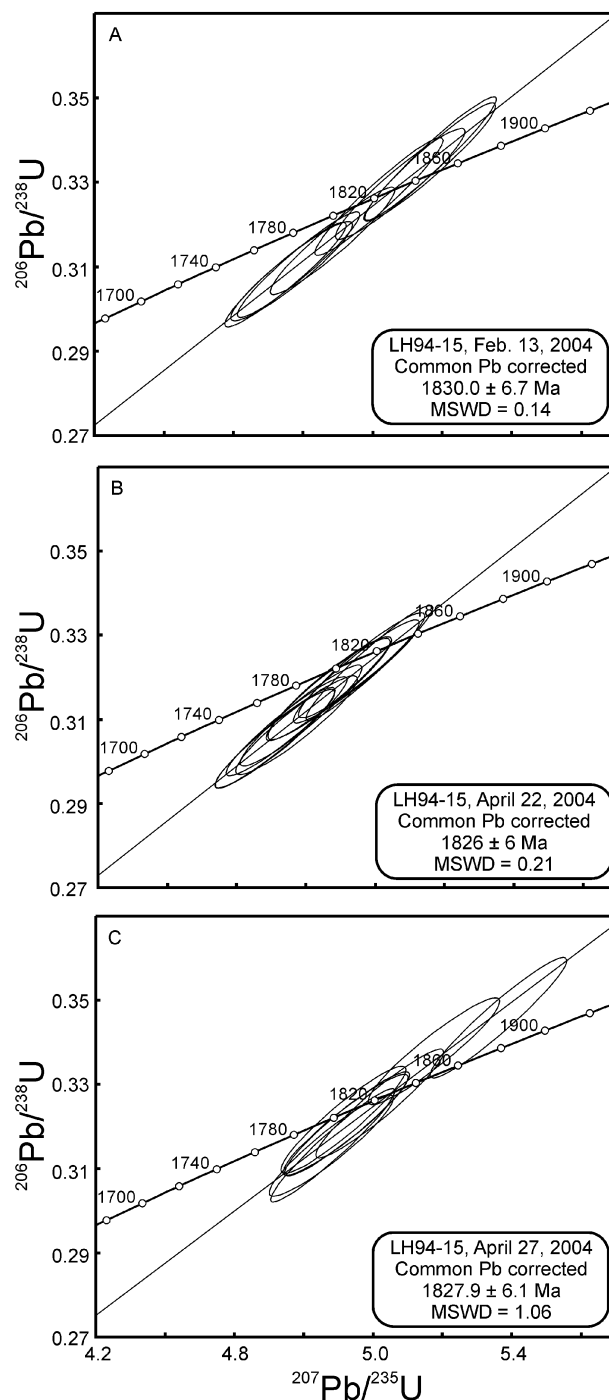


**Fig. 5** Concordia diagrams illustrating the ablation results (Tl-doped) for in-house zircon standard LH94-15 on (A) February 13th, (B) April 22nd, and (C) April 27th, 2004. These Concordia plots and subsequent Concordia diagrams (Figs. 6 and 7) were produced with Isoplot.<sup>43</sup> Error ellipses are at the  $2\sigma$  level.

contrary to several previous LA-ICP-MS investigations (*e.g.*, ref. 22), a statistical analysis for the purpose of rejecting data points was not conducted here—all analyzed data are used for age calculation. The excellent reproducibility and accuracy of the  $^{207}\text{Pb}/^{206}\text{Pb}$  values recorded for LH94-15, BR266 and 91500 zircons validates the Tl-doping technique employed here to monitor for instrumental mass bias. The high quality of the Pb isotopic data produced in this study is also demonstrated in Fig. 6. This diagram plots the total amount of Pb (nanograms) ablated from the two international zircon standards BR266 and 91500 used in this study and the typical uncertainty ( $\%$ ,  $2\sigma$ ) associated with the  $^{207}\text{Pb}/^{206}\text{Pb}$  value for an individual laser ablation analysis. These values are compared with those



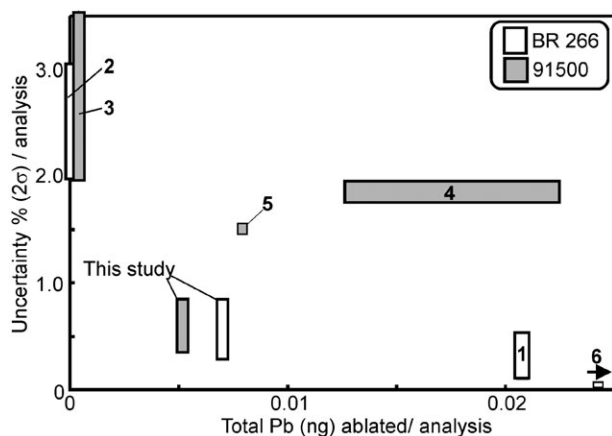


**Fig. 6** Comparative plot illustrating the typical uncertainty (internal precision,  $2\sigma$  level) associated with the  $^{207}\text{Pb}/^{206}\text{Pb}$  measurement versus the total amount of Pb (ng) ablated for BR266 and 91500 using various laser ablation-ICP-MS configurations and SHRIMP analysis. 1, MC-ICP-MS (all Faraday configuration—IsoProbe Instrument, Simonetti *et al.*, unpublished BR266 data; 2, SHRIMP;<sup>23</sup> 3, LA-quadrupole;<sup>19</sup> 4, LA-quadrupole;<sup>22</sup> 5, LA-quadrupole;<sup>2</sup> 6, range of  $\sim 3$ –11 ng of total Pb by ID-TIMS.<sup>23</sup>

reported in recent laser ablation-ICP-MS, SHRIMP and ID-TIMS investigations for the same zircon standards. Fig. 6 indicates that the data obtained in this study compare extremely well, both in terms of total Pb ablated and associated internal precision per individual analysis, compared with those previously published using different instrument configurations. In addition, the amount of Pb (ng) ablated for a typical analysis of other accessory minerals, such as monazite, is several orders of magnitude higher ( $\sim 1$  ng) assuming a Pb concentration  $> 1000$  ppm and the raster area ( $60 \mu\text{m} \times 60 \mu\text{m} \times 15 \mu\text{m}$ ) employed by Horstwood *et al.*<sup>7</sup>

### 3.3. U–Pb dating unknowns and zircon populations

Fig. 7 illustrates the typical quality of U–Pb results obtained by the instrumentation and analytical protocol described herein for zircon populations characterized by a single crystallization age. HSO-334 is a sample of granodiorite collected in the Laughland Lake area, within the northern Rae domain of central mainland Nunavut (Canada). The pluton intrudes supracrustal rocks of the *ca.* 2.73–2.69 Ga Committee Bay greenstone belt.<sup>34</sup> The *ca.* 2604  $\pm$  6.9 Ma age is consistent with a widespread 2610–2580 Ma plutonic suite recognized within the Committee Bay region,<sup>34</sup> and part of a regionally extensive *ca.* 2.64–2.60 Ga suite of I-type plutons emplaced throughout the Rae domain.<sup>35</sup>

The analytical protocol described here was also tested using a population of detrital zircons recovered from a fine-grained metagreywacke sample (CB97-12) from the Lindal Bay area of the Assean Lake Crustal complex located at the northwest periphery of the Superior Province in northern Manitoba.<sup>36,37</sup> Sample CB97-12 was chosen for the comparative study since the detrital zircons were previously dated using both ID-TIMS<sup>36</sup> and SHRIMP<sup>37</sup> methods. The sample of metagreywacke (CB00-56) investigated here by LA-MC-ICP-MS analysis was taken from the same location as that for sample CB97-12.

All of the 10 abraded zircon grains previously analyzed by ID-TIMS yielded  $^{207}\text{Pb}/^{206}\text{Pb}$  ages between  $\sim 3.2$  to  $\sim 3.8$  Ga, with one low-U zircon grain recording a concordant age of  $3749 \pm 1$  Ma.<sup>36</sup> The U–Pb results from the more detailed SHRIMP study of sample CB97-12 (Böhm *et al.*<sup>37</sup>) are shown in Fig. 8A; these indicate once again that the Lindal Bay metagreywacke sampled crust with ages ranging from  $\sim 3.2$  to  $\sim 3.9$  Ga and thus confirm the ID-TIMS results. In Fig. 8B,

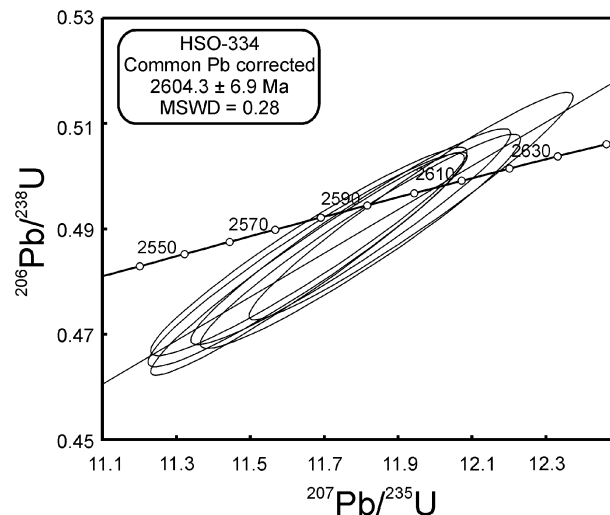


**Fig. 7** Concordia diagram for sample HSO-334 based on the laser ablation analysis (TI-doping) of 6 individual grains. The Pb and U concentrations determined by ID-TIMS for zircons from sample HSO-334 are approximately 200 ppm and 100 ppm, respectively. Ellipses are at the  $2\sigma$  level.

the results obtained by laser ablation-MC-ICP-MS are illustrated for comparison. Fig. 8B clearly shows that the distribution of U–Pb ages determined by LA-MC-ICP-MS is identical with those determined by previous SHRIMP<sup>37</sup> (Fig. 8A) and ID-TIMS<sup>36</sup> investigations for the same sample.

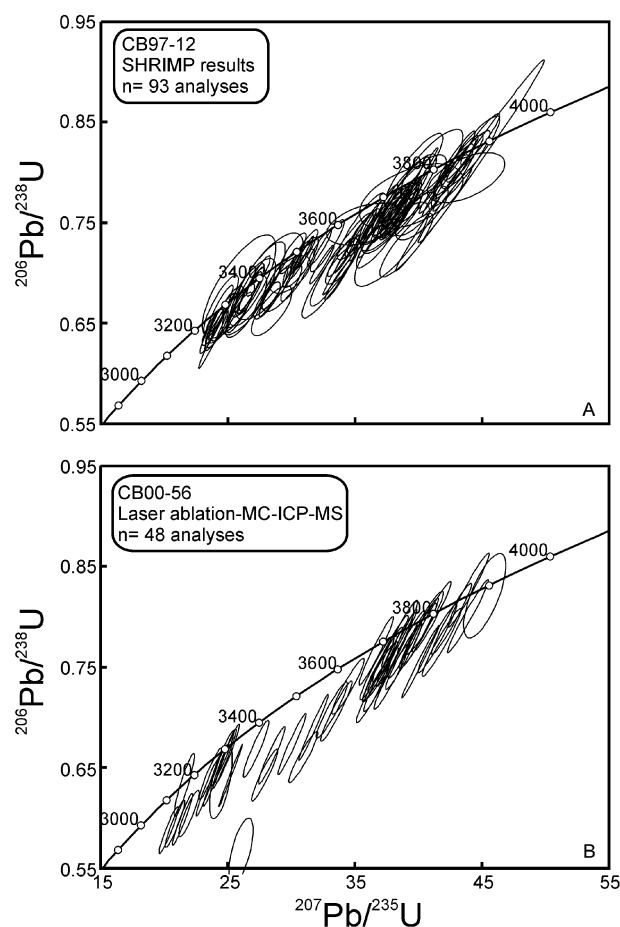


**Fig. 8** Concordia diagrams illustrating U–Pb results for sample (A) CB97-12 obtained by SHRIMP (at the Geological Survey of Canada, Ottawa)<sup>37</sup> and (B) sample CB00-56 taken from the same outcrop location and analyzed by LA-MC-ICP-MS (several years later) using the TI-doping analytical protocol developed here. Ellipses are at  $2\sigma$  level.

#### 4. Summary

The relative standard deviation ( $2\sigma$ ) associated with the Pb/U values is similar (or slightly better depending on the absolute count rate) to that reported in laser ablation-MC-ICP-MS studies employing a “raster” mode of analysis.<sup>7</sup> However, rastering consumes  $\sim 3$  times more sample volume per analysis, e.g. ref. 7, compared with the protocol employed in this study. The U versus Pb inter-element fractionation during a laser ablation run is dependent on many factors, including laser wavelength, pulse width and energy, particle size distribution and beam profile,<sup>38–41</sup> the relative importance of these factors is still a matter of much debate. Liu *et al.*<sup>42</sup> state that stoichiometric ablation for U/Pb measurements using a 213 nm laser system is achieved when laser irradiance is  $>0.6$  GW cm<sup>-2</sup>. The corresponding laser irradiance used during our experiments is slightly lower at  $\sim 0.1$ – $0.12$  GW cm<sup>-2</sup>, and thus may limit the relative standard deviation associated with the U/Pb values during one analytical session.

We report accuracies and internal precisions for ‘average’ zircons comparable to or better than those generated by more expensive systems such as sensitive high-resolution ion microprobes (SHRIMP). However, the final quality of the analyses is also a function of the quality of zircons hand-picked for analysis, the homogeneity of the standard used for the normalization procedure, the quality of the ion counters, and the general level of ‘cleanliness’ maintained for isotopic standard solutions, laser ablation cell and ion transfer optics of the instrument. The results from this study indicate that for research investigations focusing on the dating of a large population of zircon grains ( $>50$ ), it would certainly prove more cost effective and time efficient to use the analytical protocol described here than either ID-TIMS or SHRIMP. In addition, we demonstrate that the TI-doping method is slightly advantageous for analyzing large detrital zircon populations compared with the matrix-matching technique.

#### Acknowledgements

The radiogenic isotope facility at the University of Alberta is supported by a NSERC Major Facility Access grant. We thank Phil Freedman, Andy Burrows and colleagues at Nu Instruments for their hard work, discussions and for ultimately making the idea of a multiple ion counting system for radiogenic Pb on the NuPlasma a reality. The comments and reviews provided by anonymous reviewers are much appreciated and have greatly improved the quality of the manuscript.

#### References

- I. Horn, R. L. Rudnick and W. F. McDonough, *Chem. Geol.*, 2000, **164**, 281–301.
- T. E. Jeffries, J. Fernandez-Suarez, F. Corfu and G. Gutierrez-Alonso, *J. Anal. At. Spectrom.*, 2003, **18**, 847–855.
- S. E. Jackson and D. Günther, *J. Anal. At. Spectrom.*, 2003, **18**, 205–212.
- S. Jackson, N. Pearson and W. Griffin in *Laser-Ablation-ICP-MS in the Earth Sciences—Principles and Applications*, ed. P. Sylvester, Min. Ass. Can. Short Course Series, 2001, p. 29.
- M. Bizzarro, A. Simonetti, R. K. Stevenson and J. David, *Geology*, 2002, **30**, 771–774.
- S. S. Schmidberger, A. Simonetti and D. Francis, *Chem. Geol.*, 2003, **199**, 317–329.
- M. S. A. Horstwood, G. L. Foster, R. R. Parrish, S. R. Noble and G. M. Nowell, *J. Anal. At. Spectrom.*, 2003, **18**, 837–846.
- P. Vermeesch, *Earth Planet. Sci. Lett.*, 2004, **224**, 441–451.
- K. N. Sircombe and R. A. Stern, *Geochim. Cosmochim. Acta*, 2002, **66**, 2379–2397.
- C. M. Valeriano, N. Machado, A. Simonetti, C. S. Valladares, H. J. Seer and L. S. A. Simões, *Precambrian Res.*, 2004, **130**, 27–55.
- Nu Instruments, www.nu-ins.com, May 30, 2005.
- W. Todt, R. A. Cliff, A. Hanser and A. W. Hofmann, *Geophys. Mongr. Am. Geophys. Union*, 1996, **95**, 429–437.
- R. N. Taylor, T. Warneke, J. A. Milton, I. W. Croudace, P. E. Warwick and R. W. Nesbitt, *J. Anal. At. Spectrom.*, 2003, **18**, 480–484.
- L. P. Dunstan, J. W. Gramch, I. L. Barnes and W. C. Purdy, *J. Res. Natl. Bur. Stand.*, 1980, **85**, 1–10.
- S. J. G. Galer and W. Abouchami, *Mineral. Mag.*, 1998, **62A**, 491–492.
- M. Rehkämper and K. Mezger, *J. Anal. At. Spectrom.*, 2000, **15**, 1451–1460.
- M. F. Thirlwall, *Chem. Geol.*, 2002, **184**, 255–279.
- J. Košler, H. Fönneland, P. Sylvester, M. Turbet and R.-F. Pedersen, *Chem. Geol.*, 2002, **182**, 605–618.
- R. A. Cox, D. H. C. Wilton and J. Košler, *Can. Mineral.*, 2003, **41**, 307–320.
- R. E. Russo, X. L. Mao, O. V. Borisov and H. Liu, *J. Anal. At. Spectrom.*, 2000, **15**, 1115–1120.
- S. M. Eggins, L. P. J. Kinsley and J. M. G. Shelley, *Appl. Surf. Sci.*, 1998, **127–129**, 278–286.
- S. E. Jackson, N. J. Pearson, W. L. Griffin and E. A. Belousova, *Chem. Geol.*, 2004, **211**, 47–69.
- R. Stern, Geological Survey of Canada, Current Research 2001-F1, 2001.
- R. Stern and Y. Amelin, *Chem. Geol.*, 2003, **197**, 111–142.
- M. Wiedenbeck, P. Allé, F. Corfu, W. L. Griffin, M. Meier, F. Oberli, A. Von Quadt, J. C. Roddick and W. Spiegel, *Geostand. Newsl.*, 1995, **19**, 1–23.
- K. E. Ashton, L. M. Heaman, J. F. Lewry, R. P. Hartlaub and R. Shi, *Can. J. Earth Sci.*, 1999, **36**, 185–208.
- T. Munasinghe and C. B. Dissanayake, *Econ. Geol.*, 1981, **76**, 1216–1225.
- A. Kröner, I. S. Williams, W. Compston, N. Baur, P. W. Vitanage and L. R. K. Perrera, *J. Geol.*, 1987, **95**, 775–791.
- J. S. Stacey and J. D. Kramers, *Earth Planet. Sci. Lett.*, 1975, **26**, 207–223.
- K. J. R. Rosman and P. D. P. Taylor, *J. Anal. At. Spectrom.*, 1999, **14**, 5–25.
- R. H. Steiger and E. Jäger, *Earth Planet. Sci. Lett.*, 1975, **6**, 15–25.
- K. R. Ludwig, *U.S. Geological Survey Revision of Open-File Report 91-445*, 1994.
- J. D. Woodhead and J. M. Hergt, *Geostand. Newsl.*, 2001, **25**, 261–266.
- T. Skulski, H. Sandeman, M. Sanborn-Barrie, T. G. MacHattie, M. Young, C. Carson, R. Berman, D. Panagapko, D. Byrne and C. Deyell, Geological Survey of Canada, Current Research 2003-C22, 2003.
- A. N. LeCheminant and J. C. Roddick, Geological Survey of Canada, Paper 90-2, 1991.
- C. Böhm, L. M. Heaman, R. A. Creaser and M. T. Corkery, *Geology*, 2000, **28**, 75–78.
- C. O. Böhm, L. M. Heaman, R. A. Stern, M. T. Corkery and R. A. Creaser, *Precambrian Res.*, 2003, **126**, 55–94.
- A. J. G. Mank and P. R. D. Mason, *J. Anal. At. Spectrom.*, 1999, **14**, 1143–1153.
- D. Günther and C. A. Heinrich, *J. Anal. At. Spectrom.*, 1999, **14**, 1363–1368.
- N. Machado and A. Simonetti in *Laser-Ablation-ICP-MS in the Earth Sciences—Principles and Applications*, ed. P. Sylvester, Min. Ass. Can. Short Course Series, 2001, p. 29.
- M. Guillong and D. Günther, *J. Anal. At. Spectrom.*, 2002, **8**, 831–837.
- H. Liu, O. V. Borisov, X. M. Mao, S. Shuttleworth and R. E. Russo, *Appl. Spectrosc.*, 2000, **54**, 1435–1442.
- K. R. Ludwig, Berkeley Geochronological Center Spec. Publ. no. 4, 2000.